

See discussions, stats, and author profiles for this publication at: <https://www.researchgate.net/publication/267871786>

Tetrahydroxanthene-1,3(2H)-dione Derivatives from *Uvaria valderramensis*

ARTICLE in JOURNAL OF NATURAL PRODUCTS · DECEMBER 2014

Impact Factor: 3.8 · DOI: 10.1021/np500538c · Source: PubMed

CITATIONS

2

READS

39

11 AUTHORS, INCLUDING:



Allan Patrick G. Macabeo

University of Santo Tomas

58 PUBLICATIONS 208 CITATIONS

SEE PROFILE



Attila Mándi

University of Debrecen

74 PUBLICATIONS 526 CITATIONS

SEE PROFILE



Grecebio Jonathan Duran Alejandro

University of Santo Tomas

40 PUBLICATIONS 116 CITATIONS

SEE PROFILE



Scott Franzblau

University of Illinois at Chicago

359 PUBLICATIONS 8,366 CITATIONS

SEE PROFILE

Tetrahydroxanthene-1,3(2H)-dione Derivatives from *Uvaria valderramensis*

Allan Patrick G. Macabeo,^{*,†} Franze Perry A. Martinez,[†] Tibor Kurtán,[‡] László Tóth,[‡] Attila Mándi,[‡] Sebastian Schmidt,[§] Jörg Heilmann,[§] Grecebio Jonathan D. Alejandro,[⊥] Matthias Knorn,^{||} Hans-Martin Dahse,[#] and Scott G. Franzblau[○]

[†]Phytochemistry and Organic Synthesis Laboratory, and [⊥]Plant Sciences Laboratory, Research Center for the Natural and Applied Sciences, University of Santo Tomas, 1015 Manila, Philippines

[‡]Department of Organic Chemistry, University of Debrecen, POB 20, 4010 Debrecen, Hungary

[§]Institut für Pharmazie and ^{||}Institut für Organische Chemie, Universität Regensburg, D-93053 Regensburg, Germany

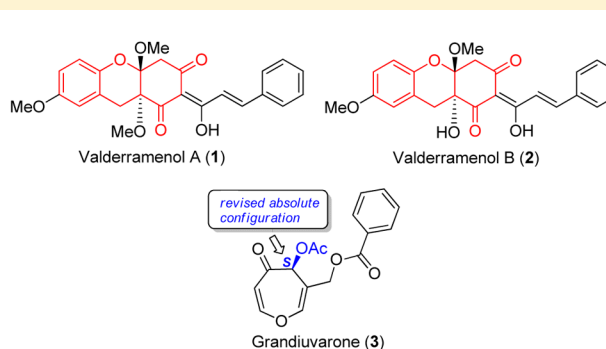
[#]Leibniz-Institute for Natural Product Research and Infection Biology, Hans-Knöll-Institute (HKI), D-07745 Jena, Germany

[○]Institute for Tuberculosis Research, College of Pharmacy, University of Illinois at Chicago, Chicago, Illinois 60612, United States

S Supporting Information



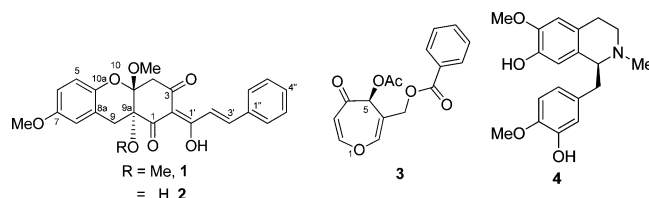
Uvaria valderramensis



ABSTRACT: Two tetrahydroxanthene-1,3(2H)-dione metabolites, valderramenols A (1) and B (2), were isolated from the Philippine endemic Annonaceous species *Uvaria valderramensis*. Planar structures of the *rac*-xanthene-1,3-(2H)-diones 1 and 2 were established by MS and NMR measurements. Their enantiomers were separated by chiral HPLC, and the absolute configurations of the separated enantiomers were determined by comparison of the HPLC-ECD spectra with computed TDDFT-generated spectra. A TDDFT-ECD study of the known grandiuarone (3) allowed the revision of its absolute configuration as *S*. Compound 1 showed antitubercular activity (MIC 10 $\mu\text{g/mL}$), while 3 and 4 had weaker activities (MIC 32 $\mu\text{g/mL}$). Oxepinone 3 exhibited cytotoxic activity against KB-562, a chronic myeloid leukemia cell line.

The genus *Uvaria* L. of the family Annonaceae comprised of more than 150 species, known to accumulate structurally interesting and bioactive compounds.¹ As part of an ongoing research program to discover new compounds from Philippine endemic plants with potential antitubercular and anticancer activity,² the chemical constituents of a newly taxonomically assigned species, *Uvaria valderramensis* Cabuang, Exconde & Alejandro, were investigated. *U. valderramensis* is a small shrub (ca. 3–7 m tall) growing in the lowlands and forests of Valderrama, Antique, Panay Island, Philippines, and is known locally as “usog” in Filipino. Its identification and distinction from other *Uvaria* species were aided by morphological and molecular phylogenetic evidence.³ Reported herein are the identification of two new xanthene-1,3-(2H)-dione derivatives, 1 and 2, along with the known compounds 3 and 4, and evaluation of their antitubercular and cytotoxic activities. The revision of the absolute configuration of (+)-grandiuarone (3)⁴ is also

presented in this paper on the basis of TDDFT-ECD calculations.



The molecular formula of valderramenol A (1) was determined by HRESIMS to be $\text{C}_{25}\text{H}_{24}\text{O}_7$, implying 14 degrees of unsaturation, based on its sodiated molecular ion peak (m/z 459.1414 $[\text{M} + \text{Na}]^+$, calcd 459.1419 for $\text{C}_{25}\text{H}_{24}\text{O}_7\text{Na}$). The IR

Received: July 2, 2014

Published: November 5, 2014

spectrum showed bands at 1666 and 1575 cm^{-1} , corresponding to a conjugated ketone and a hydrogen-bonded conjugated ketone moiety, respectively. The ^1H NMR spectrum of **1** showed signals due to two isolated diastereotopic methylenes (δ_{H} 3.26, H-4 β ; 3.28, H-4 α ; 3.01, H-9 β ; 3.69 H-9 α), three methoxy groups (δ_{H} 3.35, OMe-4a; 3.33, OMe-9a; 3.76, OMe-7), two *trans*-olefinic protons (δ_{H} 8.17, H-2'; 7.97, H-3'), eight aromatic protons (δ_{H} 7.37–7.62, H-2'' to 6''; 6.67–6.73, H-8, H-5, H-6), and an enolic (OH) proton at δ_{H} 18.40 indicative of a strong intramolecular H-bond (Table 1). The ^{13}C NMR spectrum

Table 1. NMR Spectroscopic Data (CDCl_3 , 600 MHz) for Valderramenols A (**1**) and B (**2**)

position	1			2	
	^1H	^{13}C	HMBC ^a	^1H	^{13}C
1		190.9			191.9
2		108.5			108.3
3		199.0			198.2
4 β	3.26 d (18)	39.4	3, 4a, 9a	3.20 d (17.9)	39.6
4 α	3.28 d (18)		4a	3.30 d (17.9)	
5	6.73 d (8.8)	117.5	8a, 10a	6.78 d (8.8)	117.6
6	6.67 dd (3, 8.8)	113.7	10a	6.69 dd (3, 8.8)	114.1
7		154.7			154.6
8	6.73 d (3)	113.4	8a, 10a	6.65 d (3)	113.2
9 β	3.01 d (15)	24.9	1, 8a, 9a	2.98 d (15.9)	32.2
9 α	3.69 d (15)		8, 8a, 4a, 9a	3.69 d (15.9)	
4a		97.2			97.5
8a		122.3			121.6
9a		79.2			74.6
10a		143.8			144.3
1'		187.6			188.2
2'	8.17 d (16)	121.5	1', 1''	8.17 d (16)	121.1
3'	7.97 d (16)	146.9	1', 2''/6''	7.99 d (16)	147.1
1''		134.7			134.7
2''/6''	7.37 d (7.5)	128.0	1'', 3''/5''	7.40 m	128.9
3''/5''	7.62 dd (7.5, 8)	129.1	2''/6'', 4''	7.64 m	129.2
4''	7.37 d (8)	131.1	3''/5''	7.40 m	131.2
OMe-7	3.76 s	55.5	7	3.75 s	55.6
OMe-4a	3.35 s	49.2	4a	3.44 s	49.8
OMe-9a	3.33 s	52.2	9a		
OH-9a				3.42 s	
OH-1'	18.40 brs		2, 3, 1', 2'	18.40 brs	

^aHMBC correlations, optimized for 10 Hz, are from proton(s) stated to the indicated carbon.

displayed 25 carbon signals including those for three ketonic/enolic carbons (δ_{C} 187.6, 190.9, 199.0), an acetal carbon (δ_{C} 97.2), three methoxy carbons (δ_{C} 49.2, 52.2, 55.5), an oxygenated sp^3 carbon (δ_{C} 79.2), two sp^3 methylenes (δ_{C} 24.9, 39.4), two oxygenated sp^2 carbons (δ_{C} 143.8, 154.7), three olefinic carbons (δ_{C} 121.5, 146.9, 108.5), and 10 aromatic carbons (δ_{C} 113.4–134.7) (Table 1). Analysis of the ^1H – ^1H COSY and HSQC spectra disclosed partial structures (Figure 1, bold line) corresponding to an olefin (C-2'–C-3'), a two-proton-coupled system of an aromatic moiety (C-5–C-6), and a monosubstituted benzene structure (C-2–C-3–C-4–C-5–C-6). The remaining connections were established through key correlations observed in the HMBC spectrum (Figure 1a). The H-3'/C-1' and H-2'/C1'' correlations allowed a determination of the connection of the styryl moiety to the enol functionality

and hence the position of the enol group. A benzopyran substructure (rings A and B) was established through key correlations observed in H-6/C-10a, H-5/C8a, H-8/C7, H-8/C-10a, H-9 α /C-8, H-9 α /C-4a, H-9 α /C-9a, H-9 α /C-10a, H-9 β /C-8a, and H-9 β /C-9a. The annelation of a β -triketone unit (ring C) to ring B enabled the construction of an oxidized xanthene moiety, which was made possible by correlations noted in H-9 α /C-4a, C-9a, H-9 β /C-9a, H-9 β /C-1, H-4 α , H-4 β /C-3 and H-4 α , H-4 β /C-4a, and H-4 α /C-2. The 3H singlets assigned at δ_{H} 3.35 and 3.33 with C-4a and C-9a, respectively, along with the proton signal at δ_{H} 3.76 with C-7 showed the location of the methoxy groups. Finally, the structure of **1** was fully elucidated through a key HMBC correlation of the 1'-enolic hydroxy proton with C-2 and C-3, thus corroborating a xanthene scaffold connected to an enolized cinnamoyl moiety.

The relative configuration of valderramenol A (**1**) was determined by analysis of coupling constants and NOESY correlations. The *E* configuration for C-2' and C-3' was deduced from the 16 Hz coupling constant ($^3J_{\text{HH}}$).⁵ The absence of a spatial correlation between OMe-4a (methyl acetal) and OMe-9a suggested a *trans*-orientation corresponding to a (4a*S**, 9a*R**) relative configuration for **1**, which was confirmed by NOE correlations between H-9 β and OMe-4a and H-9 α and OMe-9a. On the basis of the analysis of spectroscopic data of **1**, the structure 2-[(*E*)-1-hydroxy-3-phenylallylidene]-4a,7,9a-trimethoxy-4,4a,9,9a-tetrahydro-1*H*-xanthene-1,3(2*H*)-dione was determined. The structure of **1** has a similarity to cyathoviridine, a related derivative from *Cyathostemma viridiflorum*,⁶ and to oxymitron, a C-7 demethoxy congener with C-4a/C-9a *cis* stereochemistry from *Oxymitra kingii*,⁷ with both plant species belonging to the family Annonaceae. On the basis of the NMR spectroscopic data of **1** obtained under similar conditions to that of cyathoviridine, valderramenol A (**1**) could be a C-3 tautomer of cyathoviridine.

Compound **1** gave a zero specific rotation and showed a baseline ECD curve suggesting that it is a racemic mixture. This was confirmed also by chiral HPLC analysis, which afforded two baseline-separated peaks with Chiralpak IC stationary phase using hexane– CH_2Cl_2 (70:30) as mobile phase. The two peaks had opposite signs of optical rotations in the HPLC-ORD chromatogram, and mirror image HPLC-ECD spectra (Figure 2) were recorded confirming their enantiomeric relationship. For the configurational assignment of the separated enantiomers, TDDFT-ECD calculations were carried out on the arbitrarily chosen (4a*S*, 9a*R*, 2*Z*, 2'*E*)-**1** stereoisomer for comparison with the HPLC-ECD spectra, which has been proven earlier as an efficient method to determine the absolute configuration of separated stereoisomers of bioactive synthetic⁸ and natural derivatives^{9,10} on the basis of their HPLC-ECD spectra.

The reoptimization of the initial MMFF conformers of (4a*S*, 9a*R*, 2*Z*, 2'*E*)-**1** at the B3LYP/6-31G(d) level in vacuo afforded two conformers with comparable populations (50.4% and 48.9%), which differed only in the orientation of the C-7 methoxy group (Figure 1b). The OMe-4a and OMe-9a groups both adopted an axial orientation, and the orientation of the conjugating side-chain was fixed by the strong intramolecular hydrogen bonding between the 1-carbonyl and OH-1' groups. TDDFT-ECD calculations were carried out on the two conformers at the B3LYP, BH&HLYP, and PBE0 levels of theory, applying a TZVP basis set. ECD spectra calculated in the gas phase for the gas-phase-optimized structures gave good agreement with the experimental HPLC-ECD spectrum of the first-eluting enantiomer, having a negative long-wavelength

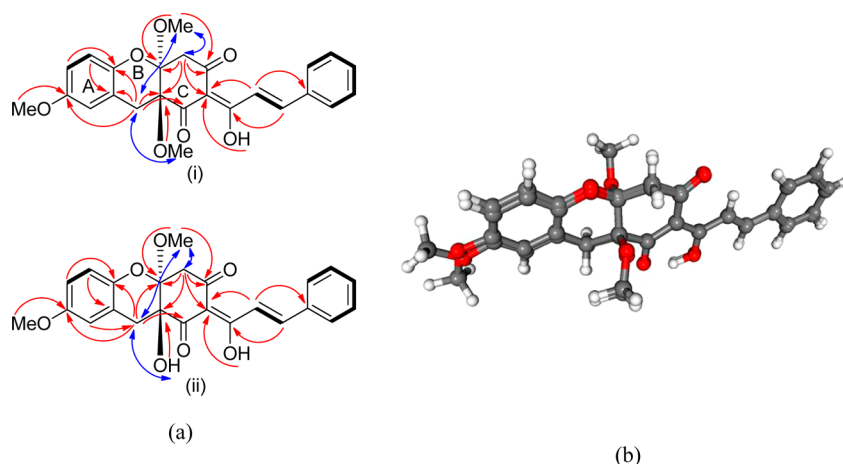


Figure 1. (a) Connectivities deduced by the COSY spectra (bold line), HMBC correlations (\rightarrow , red), and NOESY (\leftrightarrow , blue) observed for compounds **1** (i) and **2** (ii). (b) Overlaid low-energy conformers (50.4% and 48.9%) of (4aS,9aR,2Z,2'E)-**1** optimized at the B3LYP/6-31G(d) level in vacuo.

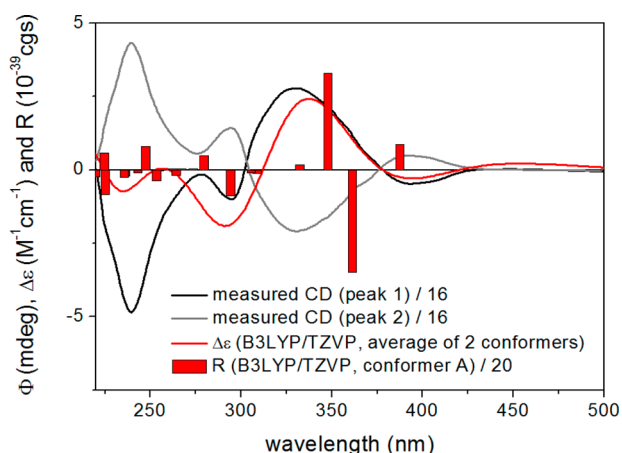


Figure 2. Experimental [HPLC-ECD; first-eluting enantiomer (black), second-eluting enantiomer (gray)] and B3LYP/TZVP-calculated spectra (red) of **1** computed for the B3LYP/6-31G(d)-optimized conformers of (4aS,9aR,2Z,2'E)-**1**.

Cotton effect (CE) above 370 nm. PCM ($CHCl_3$) solvent model ECD calculations carried out on the B97D/TZVP-optimized structures could not improve further the agreement found.¹¹ Thus, the absolute configuration of the first-eluting enantiomer of **1** with negative long-wavelength CE was determined as (4aS,9aR,2Z,2'E)-**1**.

The molecular formula of valderramenol B (**2**) was assigned as $C_{24}H_{16}O_7$ on the basis of its HRESIMS data (m/z 445.1258 [$M + Na$] $^+$ for $C_{24}H_{22}O_7Na$, calcd 445.1263). The IR spectrum showed bands at 3373 cm^{-1} (broad) for a hydroxy group, at 1668 cm^{-1} for a conjugated enol, and at 1575 cm^{-1} for an aromatic functionality. The 1H and ^{13}C NMR spectra of **2** showed a close resemblance to the resonances of **1** (Table 1) highlighted by signals due to a *trans*-olefin, a monosubstituted benzene ring, two sets of isolated diastereotopic methylenes, two methoxy groups, and an enol proton signal at δ_H 18.40, with the absence of a resonance correlated to one methoxy group of the three signals of valderramenol B. A tetrahydroanthene-1,3(3*H*)-dione structure was constructed and confirmed from correlations deduced in the 2D-NMR experiments (HSQC, HMBC, and NOESY) (Figure 1a). The relative *trans*-(4aS*,9aR*) stereochemistry was deduced for the condensed chromane moiety, which was supported by observed NOE correlations of OMe-4a with H-

4 β and H-9 β , and OH-9a with H-4 α . Similar to **1**, valderramenol B (**2**) had a zero specific rotation and showed a baseline ECD curve indicating that it is also a racemic compound. Thus, the structure (4aS*,9aR*,2Z)-9a-hydroxy-2-[(*E*)-1-hydroxy-3-phenylallylidene]-4a,7-dimethoxy-4,4a,9,9a-tetrahydro-1*H*-xanthene-1,3(2*H*)-dione could be assigned for valderramenol B. The enantiomers of **2** could also be separated under similar chiral HPLC conditions used for valderramenol A (**1**), and the absolute configurations of the enantiomers were assigned on the basis of the elution order.

The known compounds grandiuvarone (**3**), having a chiral 4-oxepinone moiety,⁴ and the benzyloquinoline alkaloid reticuline (**4**)¹² were identified by comparison of their NMR data with literature values. This is the second reported isolation of **3** from the genus *Uvaria*, with the first report of the compound being from *U. grandiflora*.⁴ Interestingly, the two species are both classified in the same Southeast Asian *Uvaria* subclade based on molecular phylogenetic analysis.³ In addition, reticuline (**4**), a rare alkaloid in *Uvaria* having been identified only in the African species *U. acuminata* and *U. lucida*, was isolated for the first time from an Asian *Uvaria* species.¹²

The 5*R* absolute configuration of (+)-grandiuvarone (**3**) has been reported earlier by comparing its negative long-wavelength CE at 316 nm with the 310 nm positive CE of (7*S*,8*R*)-leptosphaerone.¹³ The grandiuvarone sample isolated in this study showed the same ECD bands reported for (+)-grandiuvarone.¹³ However, in acetonitrile solution, an intense 202 nm negative CE was observed, which was not previously observed in methanol. In addition, additional weak CEs above 316 nm were also identified with measurements using a longer path length. Due to their difference in structures and chromophoric systems, the ECD comparison with leptosphaerone is not justified and, therefore, is prone to error. Thus, TDDFT-ECD calculations were performed on (5*S*)-**3** to determine its absolute configuration unambiguously. The initial MMFF conformers were reoptimized with B3LYP/6-31G(d) in vacuo, B3LYP/TZVP and B97D/TZVP with the PCM solvent model for acetonitrile. ECD spectra calculated using the three methods in the gas phase for the B3LYP/6-31G(d) in vacuo optimized conformers were in poor agreement with the experimental spectrum of **3**. ECD spectra calculated with a solution model for the B3LYP/TZVP (PCM/MeCN) conformers showed a significant improvement, while solution model ECD calculations for the B97D/TZVP (PCM/MeCN)-optimized conformers afforded the best agree-

ment (Figure 3).¹¹ The different types of conformational analysis revealed that the precise estimation of the geometry of the

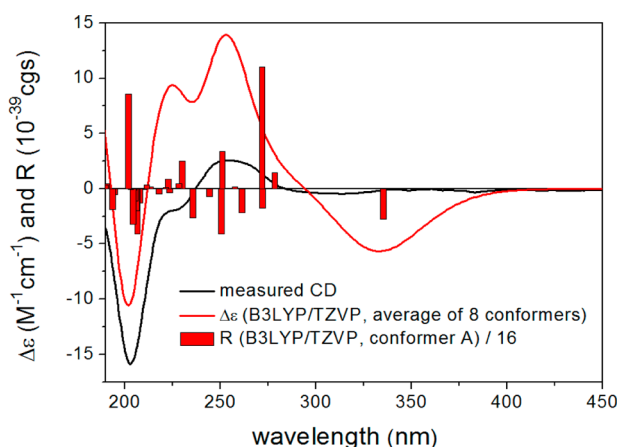


Figure 3. Experimental ECD spectrum of grandiuvarone (**3**, black) compared with the B3LYP/TZVP-calculated ECD spectrum computed for the B97D/TZVP (PCM/MeCN)-optimized conformers of (*S*)-**3**.

identified conformers and their populations requires more advanced methods and the PCM solvent model for resolution. The B97D/TZVP (PCM/MeCN) reoptimization of the initial MMFF conformers afforded eight conformers above a 1% population (Supporting Information). In the first four low-energy conformers (A–D), totaling 75.4% of the population, the oxepin-4(*SH*)-one ring adopted a slightly bent conformation with an axial OAc-5 group to reduce repulsion with the C-6 benzoate substituent. The enone chromophore had +156.4–162.9° values for the $\omega_{O,C-4,C-3,C-2}$ torsional angle with +158.1° for the lowest energy conformer (27.3%). The computed ECD spectra of the four low-energy conformers were quite similar and reproduced the measured negative lowest energy CE, although they differed in the conformation of the benzoate ester moiety. In the next four higher energy conformers (E–H), represented by 24.1% of the total population, the C-5 flipped to the other position, moving the OAc-5 group to an equatorial orientation, and the $\omega_{O,C-4,C-3,C-2}$ torsional angle varied in the range –167.0° to –167.6°. As a consequence, their computed ECD spectra were different from those of the first four low-energy conformers, and positive CEs were calculated for the lowest energy ECD transition. The Boltzmann-averaged computed ECD spectra of the eight B97D/TZVP (PCM/MeCN) solution conformers of (*S*)-**3** reproduced well the experimental spectrum, with B3LYP/TZVP giving the best agreement, which allowed the revision of the absolute configuration of (+)-grandiuvarone (**3**) as *S*.

The compounds isolated were tested for their antitubercular and cytotoxic activity using MABA¹⁴ and CellTiter-Blue¹⁵ and MTT¹⁶ assays, respectively. Among the tested compounds, **1** exhibited inhibitory activity (MIC 10 μ g/mL) followed by **3** and **4** (MIC 32 μ g/mL), while **2** was inactive against *Mycobacterium tuberculosis* H₃₇Rv. On the basis of the results for **1** and **2**, it can be deduced that a methylated OH-9a is important for antimycobacterial activity. Grandiuvarone (**3**) showed cytotoxic properties against human umbilical vein endothelial cells (HUVEC, GI₅₀ 5.4 μ g/mL) and human chronic myeloid leukemia cells (K-562, GI₅₀ 1.4 μ g/mL) with comparable activity to imatinib and doxorubicin. The cytotoxic activity of **1** and **3** is likely attributed to Michael acceptor properties of the enone moieties toward biological/cellular nucleophiles.¹⁷

EXPERIMENTAL SECTION

General Experimental Procedures. IR data were recorded using a Bio-Rad Excalibur FTS 300 spectrophotometer. ¹H and ¹³C NMR data were acquired with a Bruker 600 MHz Kryto spectrometer using solvent signals (CDCl₃; δ_H 7.26/ δ_C 77.6) as references. The HSQC and HMBC experiments were optimized for 145.0 and 10.0 Hz, respectively. HRESIMS data were acquired using an Agilent Q-TOF 6540 UHD mass spectrometer. Thin-layer chromatography was performed using Merck silica gel 60 F₂₅₄ precoated plates (0.25 mm) and visualized by UV fluorescence quenching and staining with vanillin-sulfuric acid. Column chromatography was performed on Merck silica gel 60 (0.063–0.200 mm) or Merck flash silica gel 60 (0.040–0.063 mm) stationary phases. Chiral HPLC separation of **1** were performed on a JASCO HPLC system with Chiralpak IC column [5 μ m, 150 \times 4.6 mm, hexane–CH₂Cl₂ (70:30) mobile phase, 1 mL min^{–1} flow rate], and HPLC-ECD spectra were recorded in stopped-flow mode on a JASCO J-810 electronic circular dichroism spectropolarimeter equipped with a 10 mm HPLC flow cell. ECD ellipticity (Φ) values were not corrected for concentration. For an HPLC-ECD spectrum, three consecutive scans were recorded and averaged with 2 nm bandwidth, 1 s response, and standard sensitivity. The HPLC-ECD spectrum of the eluent recorded in the same way was used as background. The concentration of the injected sample was set so that the HT value did not exceed 500 V in the HT channel down to 230 nm.

Plant Material. The leaves of *Uvaria valderramensis* were collected at Baranggay Bugnay, Valderrama, Antique, Panay Island, Central Philippines (11°00'05.60" N; 122°07'45.58" E), in October 2013 and were identified and authenticated by one of the authors (G.J.D.A.). Voucher specimens (USTH VI011) were deposited at the University of Santo Tomas Herbarium (holotype) and at the Philippine National Herbarium (isotype), Manila, Philippines.

Extraction and Isolation. A CH₂Cl₂–MeOH (1:1) extract (278 g) of the ground, air-dried leaves of *U. valderramensis* (4 kg) was fractionated further into hexanes, CH₂Cl₂, and *n*-BuOH subextracts. The CH₂Cl₂ subextract (51 g) was initially purified by flash silica gel chromatography using EtOAc–hexanes and MeOH–EtOAc gradient systems (20%) to give 12 fractions. Fraction 4, eluted with 10:1 hexanes–EtOAc, was separated on a silica gel 60 column to afford compound **3** as a brownish, viscous oil (556 mg). Fraction 6, eluted with 9:1 hexanes–EtOAc, was purified on a silica gel column and afforded compounds **1** (644 mg) and **2** (9.4 mg) as yellow, amorphous solids. Alkaloid **4** was obtained as a yellowish solid (6.3 mg) after purification of fraction 10 eluted with 1:1 hexanes–EtOAc on a silica gel 60 column.

Valderramenol A (1): yellow, amorphous solid; [α]_D²³ 0 (*c* 1.0, CHCl₃); IR (KBr) ν_{\max} 2937, 1666, 1620, 1575, 1490, 1417, 1201, 1049, 1037, 935, 680 cm^{–1}; ¹H, ¹³C, and HMBC data, see Table 1; HRESIMS *m/z* 459.1414 [*M* + Na]⁺ (calcd for C₂₅H₂₄O₇Na, 459.1419).

(4*aS*,9*aR*,2*Z*,2'*E*)-1: retention time (*t*_R) 20.11 min [(Chiralpak IC, hexane–dichloromethane (70:30)]; HPLC-ECD data in hexane–dichloromethane (80:20) as λ_{\max} (Φ) 393 (–7.5), 330 (44.4), 294 (–16.0), 239 (–77.6).

(4*aR*,9*aS*,2(1*Z*,2'*E*)-1: *t*_R 23.18 min [(Chiralpak IC, hexane–dichloromethane, 70:30)]; HPLC-ECD data in hexane–dichloromethane (80:20) as λ_{\max} (Φ) 391 (7.7), 331 (–33.4), 294 (22.8), 239 (69.2).

Valderramenol B (2): yellow solid; [α]_D²³ 0 (*c* 1.0, CHCl₃); IR (KBr) ν_{\max} 3373 (br), 2929, 2831, 1668, 1618, 1575, 1492, 1423, 1205, 1038, 937, 682 cm^{–1}; ¹H and ¹³C data, see Table 1; HRESIMS *m/z* 445.1258 [*M* + Na]⁺ (calcd for C₂₄H₂₂O₇Na, 445.1263).

(4*aS*,9*aR*,2*Z*,2'*E*)-2: *t*_R 24.34 min [Chiralpak IC, hexane–dichloromethane (80:20)].

(4*aR*,9*aS*,2(1*Z*,2'*E*)-1: *t*_R 28.80 min [Chiralpak IC, hexane–dichloromethane, 80:20)].

Grandiuvarone [(S)-3]: [α]_D²³ +34 (*c* 0.1, CHCl₃; lit.⁴ +34.9); ECD (MeCN, λ [nm] ($\Delta\epsilon$), *c* = 6.04 \times 10^{–4} M) 375 (0.21), 339 (0.19), 330 (–0.15), 316 sh (–0.34), 303 (–0.37), 261sh (2.46), 252 (2.69), 226 (–2.07), 202 (–18.68).

Computational Calculations. Mixed torsional/low-mode conformational searches were carried out with MacroModel 9.9.223

software¹⁸ using the Merck molecular force field (MMFF) with an implicit solvent model for chloroform. Geometry reoptimizations at B3LYP/6-31G(d) in vacuo, B3LYP/TZVP, and B97D/TZVP, with the PCM solvent model for acetonitrile or chloroform followed by TDDFT calculations using various functionals (B3LYP, BH&HLYP, PBE0), and the TZVP basis sets were performed with the Gaussian 09 package.¹⁹ ECD spectra were generated as the sum of Gaussians with 3000 and 3600 cm⁻¹ half-height widths (corresponding to ca. 19 and 23 at 250 nm) using dipole-velocity-computed rotational strengths.²⁰ Boltzmann distributions were estimated from the ZPVE-corrected B3LYP/6-31G(d) energies in vacuo and from the B3LYP/TZVP or B97D/TZVP energies in the solvent model calculations. The MOLEKEL software package was used for visualization of the results.²¹

Biological Assays. The antitubercular activity of the compounds against *Mycobacterium tuberculosis* H₃₇Rv was evaluated using a MABA assay with rifampin (MIC = 0.15 µg/mL), isoniazid (MIC = 0.63 µg/mL), and streptomycin (MIC = 0.83 µg/mL) as positive drug controls.¹⁴ Cytotoxicity data against the HUVEC, K-562, HeLa, T47D, MDA-231, and SK-BR-3 cell lines were obtained by the CellTiter Blue¹⁵ and MTT¹⁶ colorimetric methods with imatinib (GI₅₀ >10 µg/mL vs HUVEC; GI₅₀ 0.1 µg/mL vs K-562; CC₅₀ >10 µg/mL vs HeLa) and doxorubicin (GI₅₀ 0.1 µg/mL vs HUVEC; GI₅₀ 1.0 µg/mL vs K-562; CC₅₀ 2.0 µg/mL vs HeLa) as positive controls.

■ ASSOCIATED CONTENT

■ Supporting Information

¹H, ¹³C, and 2D-NMR spectra of compounds **1** and **2**. This material is available free of charge via the Internet at <http://pubs.acs.org>.

■ AUTHOR INFORMATION

Corresponding Author

*Tel: +63 (02) 4061611, ext. 4057. Fax: +63 (02) 7314031. E-mail: agmacabeo@mn1.ust.edu.ph.

Notes

The authors declare no competing financial interest.

■ ACKNOWLEDGMENTS

This work was funded by the Philippine Council for Health, Research and Development (PCHRD Grant No. Fp130017). T.K. thanks the Hungarian National Research Foundation (OTKA K105871) for financial support and the National Information Infrastructure Development Institute (NIIFI 10038) for the CPU time. The research of A.M. was supported by the European Union and the State of Hungary and cofinanced by the European Social Fund in the framework of TÁMOP-4.2.4.A/2-11/1-2012-0001 "National Excellence Program". Prof. D. Nagle (University of Mississippi, Oxford, MS, USA) is gratefully acknowledged for the additional cytotoxicity data.

■ REFERENCES

- (1) (a) Hufford, C. D.; Oguntimein, B. O.; Engen, D. V.; Muthard, D.; Clardy, J. *J. Am. Chem. Soc.* **1980**, *102*, 7365–7367. (b) Hufford, C. D.; Oguntimein, B. O.; Baker, J. K. *J. Org. Chem.* **1981**, *46*, 3073–3078. (c) Achenbach, H. *Pure Appl. Chem.* **1986**, *58*, 653–662.
- (2) (a) Aguinaldo, A. M.; Dalangin-Mallari, V. M.; Macabeo, A. P. G.; Byrne, L. T.; Abe, F.; Yamauchi, T.; Franzblau, S. G. *Int. J. Antimicrob. Agents* **2007**, *29*, 744–746. (b) Macabeo, A. P. G.; Vidar, W. S.; Wan, B.; Franzblau, S. G.; Chen, X.; Decker, M.; Heilmann, J.; Galvez, E.; Aguinaldo, A. M.; Cordell, G. A. *Eur. J. Med. Chem.* **2011**, *46*, 3118–31223. (c) Macabeo, A. P. G.; Avila, J. A.; Alejandro, G. J. D.; Franzblau, S. G.; Kouam, S. F.; Hussain, H.; Krohn, K. *Nat. Prod. Commun.* **2012**, *7*, 779–780.
- (3) Cabuang, P. G. D.; Exconde, B. S.; Lim, V.; Padilla, D. K. M.; Salas, S. R.; Lemana, B. O. C.; Macabeo, A. P. G.; Alejandro, G. J. D. *Philip. J. Syst. Biol.* **2012**, *6*, 1–16.

- (4) Ankisetty, S.; El-Sohly, H. N.; Li, X. C.; Khan, S. I.; Tekwani, B. L.; Smillie, T.; Walker, L. *J. Nat. Prod.* **2006**, *69*, 692–694.
- (5) Bonilla, A.; Duque, C.; Garzon, C.; Takaishi, Y.; Yamaguchi, K.; Hara, N.; Fujimoto, Y. *Phytochemistry* **2005**, *66*, 1736–1740.
- (6) Mahmood, K.; Sablé, S.; Pais, M.; Ali, H. M.; Hadi, A. H. A.; Guittet, E. *Nat. Prod. Lett.* **1993**, *3*, 245–249.
- (7) Richomme, P.; Sindbadhit, S.; David, B.; Hadi, A. H. A.; Bruneton, B. *J. Nat. Prod.* **1990**, *53*, 294–297.
- (8) Zhu, J.; Ye, Y.; Ning, M.; Mándi, A.; Feng, Y.; Zou, Q.; Kurtán, T.; Leng, Y.; Shen, J. *ChemMedChem* **2013**, *8*, 1210–1223.
- (9) Gulyás-Fekete, G.; Murillo, E.; Kurtán, T.; Papp, T.; Illyés, T.-Z.; Drahos, L.; Visy, J.; Agócs, A.; Turcsi, E.; Deli, J. *J. Nat. Prod.* **2013**, *76*, 607–614.
- (10) Gao, H.; Liu, W.; Zhu, T.; Mo, X.; Mándi, A.; Kurtán, T.; Li, J.; Ai, J.; Gu, Q.; Li, D. *Org. Biomol. Chem.* **2012**, *10*, 9501–9506.
- (11) Sun, P.; Xu, D. X.; Mándi, A.; Kurtán, T.; Li, T. J.; Schulz, B.; Zhang, W. *J. Org. Chem.* **2013**, *78*, 7030–7047.
- (12) Ichimaru, M.; Moriyasu, M.; Nishiyama, Y.; Kato, A.; Juma, F. D.; Nganga, J. N.; Ogeto, J. O. *Nat. Med.* **1997**, *51*, 272–274.
- (13) Liu, J. Y.; Liu, C. H.; Zou, W. X.; Tian, X.; Tan, R. X. *Helv. Chim. Acta* **2002**, *85*, 2664–2667.
- (14) Collins, L. A.; Franzblau, S. G. *Antimicrob. Agents Chemother.* **1997**, *41*, 1004–1009.
- (15) Krauth, K.; Dahse, H. M.; Rüttinger, H. H.; Frohberg, P. *Bioorg. Med. Chem.* **2010**, *18*, 1816–1821.
- (16) Liu, Y.; Veena, C. K.; Morgan, J. B.; Mohammed, K. A.; Jekabsons, M. B.; Nagle, D. G.; Zhou, Y. D. *J. Biol. Chem.* **2009**, *284*, 5859–5868.
- (17) Amslinger, S. *ChemMedChem* **2010**, *5*, 351–356.
- (18) MacroModel; Schrödinger LLC, 2012; <http://www.schrodinger.com/productpage/14/11/>.
- (19) Frisch, M. J.; Trucks, G. W.; Schlegel, H. B.; Scuseria, G. E.; Robb, M. A.; Cheeseman, J. R.; Scalmani, G.; Barone, V.; Mennucci, B.; Petersson, G. A.; Nakatsuji, H.; Caricato, M.; Li, X.; Hratchian, H. P.; Izmaylov, A. F.; Bloino, J.; Zheng, G.; Sonnenberg, J. L.; Hada, M.; Ehara, M.; Toyota, K.; Fukuda, R.; Hasegawa, J.; Ishida, M.; Nakajima, T.; Honda, Y.; Kitao, O.; Nakai, H.; Vreven, T.; Montgomery, J. A.; Peralta, J. E.; Ogliaro, F.; Bearpark, M.; Heyd, J. J.; Brothers, E.; Kudin, K. N.; Staroverov, V. N.; Kobayashi, R.; Normand, J.; Raghavachari, K.; Rendell, A.; Burant, J. C.; Iyengar, S. S.; Tomasi, J.; Cossi, M.; Rega, N.; Millam, J. M.; Klene, M.; Knox, J. E.; Cross, J. B.; Bakken, V.; Adamo, C.; Jaramillo, J.; Gomperts, R.; Stratmann, R. E.; Yazyev, O.; Austin, A. J.; Cammi, R.; Pomelli, C.; Ochterski, J. W.; Martin, R. L.; Morokuma, K.; Zakrzewski, V. G.; Voth, G. A.; Salvador, P.; Dannenberg, J. J.; Dapprich, S.; Daniels, A. D.; Farkas, O.; Foresman, J. B.; Ortiz, J. V.; Cioslowski, J.; Fox, D. J. *Gaussian 09*, Revision B.01; Gaussian, Inc.: Wallingford, CT, 2010.
- (20) Stephens, P. J.; Harada, N. *Chirality* **2010**, *22*, 229–233.
- (21) Varetto, U. *MOLEKEL 5.4*; Swiss National Supercomputing Centre: Manno, Switzerland, 2009.

■ NOTE ADDED AFTER ASAP PUBLICATION

An incorrect structure for compound **4** appeared in the version posted on Nov 5, 2014. The correct structure appears in the version posted on Nov 20, 2014.